NANOSYSTEMS: PHYSICS, CHEMISTRY, MATHEMATICS, 2021, 12 (3), P. 311–316

Ultraviolet and visible reflective TiO_2/SiO_2 thin films on silicon using sol-gel spin coater

S. Saravanan, R. S. Dubey

Advanced Research Laboratory for Nanomaterials & Devices, Department of Nanotechnology,
Swarnandhra College of Engineering & Technology, Narsapur-534 280, West Godavari (A.P.), India

shasa86@gmail.com

DOI 10.17586/2220-8054-2021-12-3-311-316

TiO_2/SiO_2 alternative thin films (stacks) were deposited on silicon substrates using sol-gel spin-coating techniques. The prepared samples had their corresponding optical properties analyzed by UV-Visible spectrophotometry (UV-Vis), X-ray diffractometry (XRD), a surface profilometer, and Raman spectroscopy. The optical and crystallization properties of thin films were varied and compared by changing the number of stacks. UV-Vis spectrum showed high reflectance and shifting towards the infrared region with effect of increased TiO_2/SiO_2 stacks. XRD spectra confirmed the existence of anatase TiO_2 and SiO_2 diffraction peaks. The multilayer film thickness was calculated at 109 and 151 nm at two and four stacks by a surface profilometer. The Raman spectra confirmed the Si–O–Si and TiO_2 stretching modes at 2600, 980, and 519 cm^{-1}. This investigation reveals the promising and effective UV-Visible reflective property of alternative TiO_2/SiO_2 thin films on a silicon substrate.

Keywords: Sol-gel, reflectance, multilayer, anatase, thickness.

Received: 12 November 2020

Revised: 20 March 2021

1. Introduction

Thin films could find a significant role in various semiconductor industrial applications. Numerous oxide combinations are extensively useful to improve optical (or surface) performance, such as TiO_2/SiO_2, Al_2O_3/SiO_2, ZnO/SiO_2 and ZnO/ZrO_2. In solar cells, the highest quantity of light absorption convert is possible by selecting a good combination of anti-reflection coatings materials and synthesis methods. Among the various materials, TiO_2/SiO_2 has been in demand due to its highest refractive index contrast, good passivity and providing conductive pathway [1, 2]. The formations of various metal oxide thin film and their stabilities determined by the selection of the materials [3]. The metallic coatings on multiple substrates are useful to obtain higher ultraviolet (UV), visible, infrared (IR) reflectance like silver (Ag), aluminium (Al), etc. But, the high maintenance and fabrication cost is a major issue with metallic coatings. The ultraviolet spectral region from 100 to 400 nm and reflection of this wavelength is of great importance to human life, causing the aging of skin, sunburn, etc [4]. The UV reflector is fabricated using atmospheric pressure physical vapor depositions (AP-PVD), sol-gel spin-coating, dip-coating, plasma-enhanced chemical vapor deposition (PECVD), and wet-chemical routes and multistep procedures [5–10]. This proposed work focused on UV and Visible wavelength reflective coatings of TiO_2/SiO_2 multilayers on a silicon substrate using sol-gel spin-coating methods. Sol-gel spin-coating is the easiest way to synthesize and fabricate One-dimensional photonic crystal (1DPC) layers by tuning the synthesis (precursor concentration, temperature) and fabrication (spin speed, calcined temperature, number of layers) parameters. Venkatesh Yepuri et al. (2020) addressed the process optimization of low-cost and rapid fabrication of TiO_2/SiO_2 reflectors with 100 % reflectivity. They summarized the desired reflection band of a selected wavelength range observed by changing various parameters such as the precursor concentrations, spin speed (rpm), annealing etc. Finally, the reflection window was observed from the visible to the near infrared region with 2.5 stacks [11]. Dubey et al. (2018) fabricated visible and near-IR wavelength TiO_2/SiO_2 reflectors using a sol-gel spin coater for various light trapping management applications. The homogeneous, uniform film thickness (56 – 94 nm) and cross-section of TiO_2/SiO_2 stacks were evidenced by field emission scanning electron microscopy (FESEM). Further, the elemental peaks (Ti, Si, O) and reflectance ($\sim$ 100 %) properties were studied using energy-dispersive X-ray spectroscopy (EDX) and UV-Visible spectrophotometer [12]. Sedrati et al. (2019) fabricated the TiO_2/SiO_2 Bragg reflectors using the sol-gel dip-coating process. The Raman spectrum confirmed the anatase phase. The UV-Vis-IR range shifted towards the more extended wavelength region with the effect of doping transition metals (copper, nickel, cobalt, and chromium). Also, doping TiO_2 showed enlarged stop-band of TiO_2/SiO_2 Bragg reflectors and enhanced optical properties [13]. Zhao et al. (2019) investigated the mesoporous SiO_2 and SiO_2-TiO_2 thin films prepared by the sol-gel method. The Raman spectrum confirmed the anatase TiO_2 phase, and the UV-vis reflectance spectrum shifted towards the more extended wavelength region with the effects of transition doped metals [14]. Dubey et al. (2017) fabricated TiO_2/SiO_2 Bragg reflectors for light trapping applications using a cost-effective and straightforward sol-gel spin coating method. UV-Vis spectrum showed 90 % reflectance at 617 nm using seven distributed Bragg reflectors

(DBR) stacks based structure, and the FESEM image confirmed alternative layers of one-dimensional TiO_2 and SiO_2 thin films. This DBR structure integrated solar cell design significantly enhanced light absorption [15].

This paper deals with the optical and structural properties of TiO_2 (anatase and rutile) and SiO_2 multilayers fabricated on silicon substrates using a sol-gel spin-coater. In the second section we describe the synthetic process and fabrication of thin-film TiO_2/SiO_2 structures. UV-Vis, XRD, Raman spectroscopy results are discussed in section third and summarized the work in the fourth section.

2. Experimental approach

Synthesis and fabrication procedural steps of TiO_2/SiO_2 thin films are shown in Fig. 1. Titanium butoxide (TBOT, $Ti(OBu)_4$), tetraethyl orthosilicate (TEOS, $Si(OC_2H_5)_4$), methanol (CH_3OH), acetic acid (CH_3COOH), and deionized water (DI) are the starting chemicals used without any additional purification. For the preparation of TiO_2 and SiO_2 solutions, $Ti(OBu)_4$: CH_3OH: CH_3COOH: DI and $Si(OC_2H_5)_4$:CH_3OH: CH_3COOH in the ratios of 1.2:20:1.7 and 1.5:20:2.3 respectively.

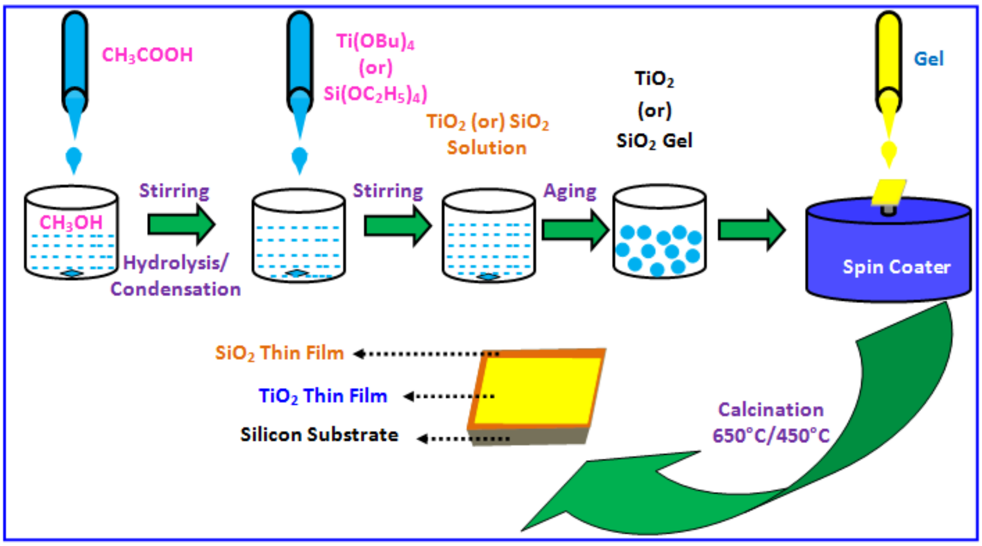

FIG. 1. The sol-gel synthesis of TiO_2 and SiO_2 thin film processing step

Initially, 1.2 ml acetic acid added in methanol (20 ml) and stirred for 5 minutes using a magnetic stirrer at room temperature. Titanium butoxide solution added drop-wise and stirring maintained for 90 minutes at room temperature (28 °C). Finally, TiO_2 solution (solution 'A') appears transparent color and was aged for 24 hrs. Next, 1.5 ml acetic acid was mixed with 20 ml methanol and stirred for five minutes with the continued dropwise addition of tetraethyl orthosilicate (2.3 ml) at 2 minutes intervals. The prepared SiO_2 solution was continuously stirred at 90 minutes (solution 'B') and aged 24 hrs. Before the deposition process, substrates were cleaned at room temperature by ultrasonication process using DI water, ethanol, and aqueous hydrofluoric (HF) acid. Using spin-coater, the alternative coating of TiO_2 and SiO_2 solution deposition coated on the glass substrates at 3000 rpm/30 sec. After the coating, thin film samples were calcined at 650 °C (TiO_2) and 450 °C (SiO_2) for 1 hour. Further, analyses were performed using the following instruments: X-ray diffractometer (XRD, Bruker D8 Advance), UV-visible spectrophotometer (UV-Vis, 1800 Shimadzu), and Surface Profilometer (SJ-301 Mitutoyo). Raman spectroscopy (micro Raman) was also used to study their optical properties.

3. Results and discussion

Figure 2 shows the reflectance spectra of 2-TiO_2/SiO_2 stacks (S1) and 4-TiO_2/SiO_2 stacks (S2) by UV-Visible spectrophotometry. Here, one alternating layer of TiO_2 and SiO_2 thin film is known as a stack. The obtained results show the high reflectance and shifted towards the longer wavelength region due to the increment of stacks. Similarly, Dubey et al. (2017) reported improved reflectance with the effect of an increased number of coating layers [15].

The enhanced reflectance could be possible in the whole UV-Visible spectrum due to the large refractive index contrast between TiO_2 and SiO_2 layers, as reported by Zhang et al. (2006) [16]. Significantly, the TiO_2 thin films could increase the reflectance in the visible and infra-red region as reported by Dalapati et al. (2015) [17]. Fig. 3 depicts

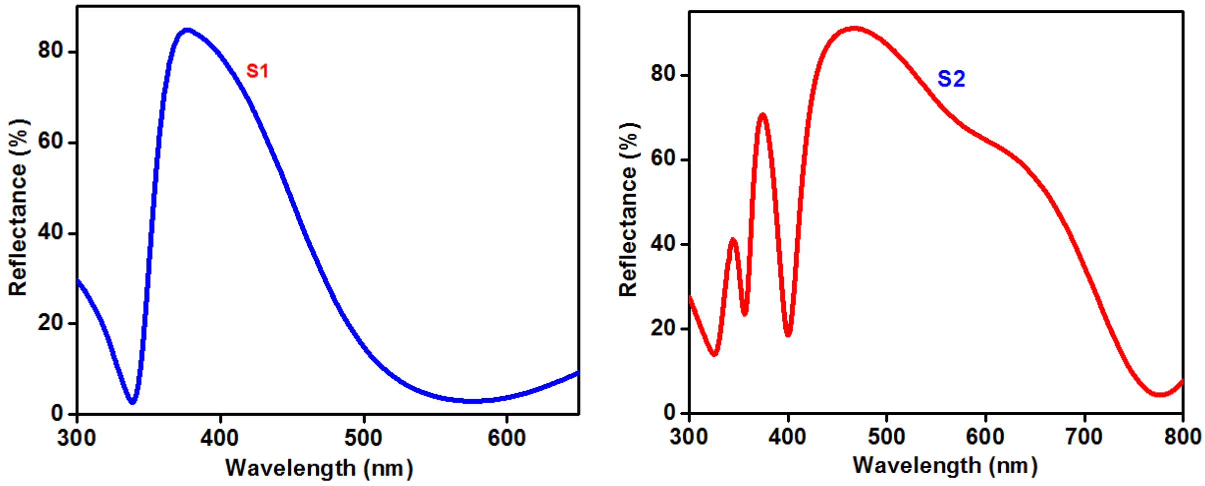

(a) (b)

FIG. 2. Reflectance spectra of two (S1) and four (S2) stacks of TiO_2/SiO_2 thin films prepared on Si substrates

the reflectance (UV-visible) fullwidth half maximum (FWHM) of samples S1 and S2 corresponding enhancement 103 and 267 nm. Here, the FWHM enhancement $\sim$ 267 nm achieved by the highest deposition layers of silicon substrate. Saravanan et al. (2019) reported work revealed the enhanced FWHM concerning the increment of stacks, and this reflectance is mainly dependent on the thickness and surface of the structure [18]. Consequently, surface profilometer techniques revealed the sample thickness of 120 nm (S1) and 160 nm (S2).

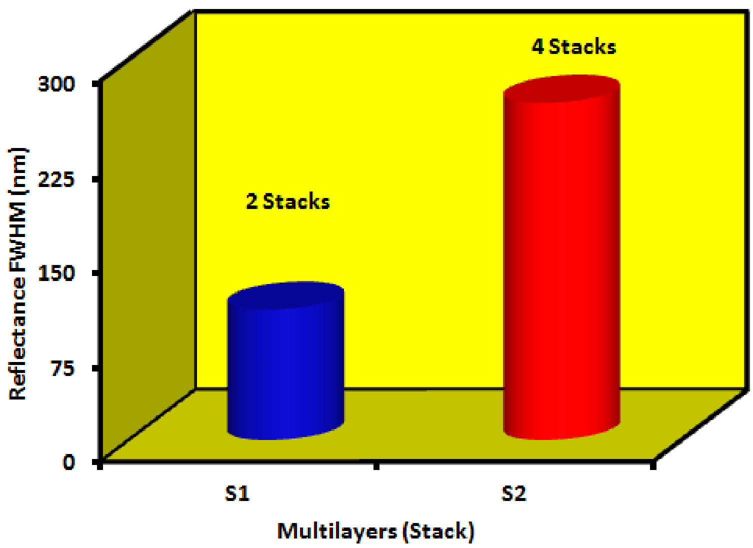

FIG. 3. Full-width half maximum (FWHM) of S1 (2 stacks) and S2 (4 stacks)

The XRD pattern can provide the structural parameters for TiO_2/SiO_2 thin films by varying the number of stacks (2-S1 and 4-S2), as shown in Fig. 4(a,b). At room temperature, thin films were fabricated which were attributed to the anatase and rutile mixed phase. The XRD patterns of the samples were noticed with the same nature. The obtained Bragg's diffraction peaks at $2\theta = 25.36°$ (A), $28.8°$ (R), $37.52°$ (A), $41.9°$ (A), $47.48°$ (A) and $53.99°$ (R) which is corresponding planes (101), (111), (004), (111), (200) and (211) respectively [11, 19]. Here, A and R are denoted as anatase and rutile peaks for our convenience. From both diffraction spectra, the intense diffraction peak noticed and confirmed the presence of anatase TiO_2 and well-matched with JCPDS#21-1272 [20–22]. The rutile diffraction can be assigned to the ICDD card #00-001-1292 and 01-072-4813. The highest TiO_2 thin film calcination temperature (650 °C) provides the rutile phase formation. Both XRD pattern, the broad and low intense peak envelope appeared

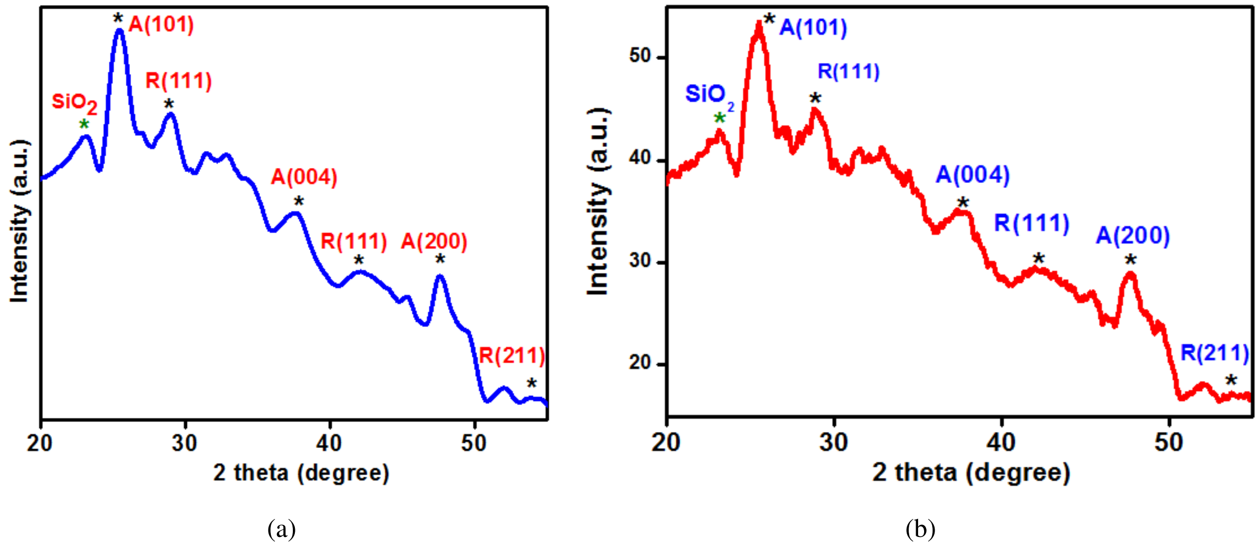

FIG. 4. XRD spectra of TiO_2/SiO_2 thin films (a) 2-stacks, S1 and (b) 4-stacks, S2

at 23°, which is attributed to the existence of amorphous silica in the prepared samples [19,23]. Finally, the impurities were not presented.

Using the Debye–Sherrer formula, the crystalline size can be calculated, ($D = k\lambda/\beta\cos\theta$), where D is the crystalline size, k is the numerical factor (0.9) referred to as the crystallite shape, λ is the X-ray incident wavelength (1.5406 Å), β is the full-width at half maximum (FWHM), and θ is the diffraction angles [24, 25]. Table 1 shows the calculated crystallite size of the samples.

TABLE 1. The crystallite size of TiO_2/SiO_2 multilayers on silicon

S.N.	Sample (TiO_2/SiO_2)	Peak positions (2θ) degree	FWHM (2θ)	Crystallite Size (nm)
1	S1 (Anatase-TiO_2)	61.75	0.1476	62.71
2	S2 (Anatase-TiO_2)	61.74	0.1476	62.70

Raman scattering is useful to identify (phase) the structural modification in 650 and 450 °C thermally treated thin film structures. Fig. 5 shows the Raman spectrum of the TiO_2/SiO_2 thin film with highest and broader intensity peaks within the range 0 to 3000 cm^{-1}. The micro Raman spectroscopy consists of the excitation wavelength, $\lambda = 785$ nm. Both spectral (S1 & S2) results showed the same nature of the spectrum by varying intensity of the peaks. First, the sharp peak at 519 cm^{-1} indicates the originating from the silicon (Si) substrate. For our convenience, Anatase, rutile, and silicon dioxide Raman modes were denoted as A, R, and S respectively. The vibrational bands of anatase TiO_2 material has centered at 137, 207, 414, 519 and 644.8 cm^{-1}, respectively, corresponding to the Raman active modes of Eg, Bg, B1g, A1g, and Eg as showed in inserted Fig. 5 [26, 27]. It can be concluded that strong anatase peak at 137 cm^{-1}. Accordingly, the normal vibrational mode of anatase bands is ΓA = 2Eg + 2Bg + B1g + A1g. The rutile TiO_2 phase identified at 238 (Eg), 450, 612. Similarly, silicon dioxide presented at 233, 333, 488 and 600 cm^{-1}. The Raman spectrum of SiO_2 had a weak peak $\sim$ 980 cm^{-1} which was attributed to the bending of Si–O–Si symmetric bond stretching [28, 29]. Finally, the broad peak at 2600 cm^{-1} indicates the presence of SiO_2. This existence of broader peaks in the Raman spectrum attribute to the electronic Raman scattering mechanism [30–32].

4. Conclusions

TiO_2/SiO_2 thin films were deposited on silicon substrates using sol-gel and spin-coating techniques. The optical properties of thin films have been studied by UV-Vis, XRD and Raman spectroscopy. UV-Vis spectroscopy showed reflectance enhancement as an effect when increasing the number of stacks. XRD and Raman spectra revealed the presence of anatase TiO_2 and amorphous silica phase in both samples. Using a surface profilometer, the thin-film

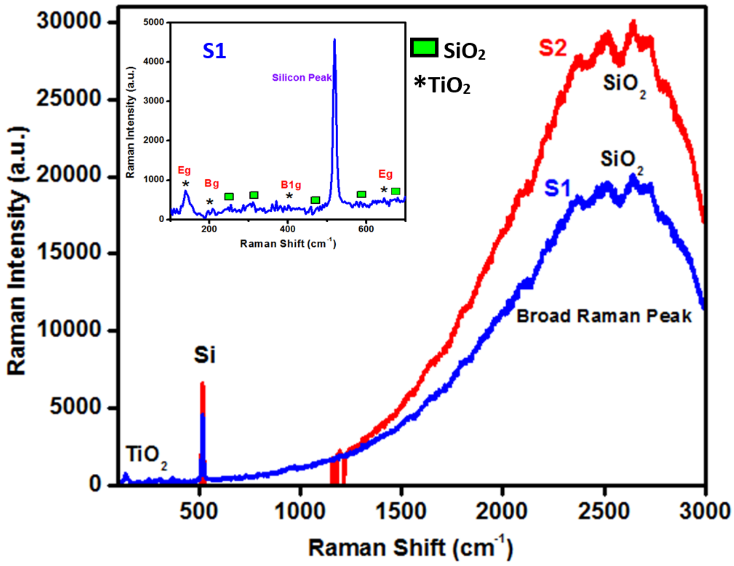

FIG. 5. Raman spectra of TiO_2/SiO_2 multilayer two stacks (S1) and four stacks (S2)

thickness of 120 nm (2 stacks) and 160 nm (4 stacks) calculated. Further, changing various parameters with optimization results will be useful for various novel applications, including solar cells, light-emitting diodes, the bandpass filters and lasers.

Acknowledgements

The authors are thankful to Mr. P. Srinivas Rao, School of Nanotechnology, Jawaharlal Nehru Technological University (JNTU), Kakinada, for availed Raman characterization. Dr. G. Ramalingam, Department of Nanoscience and Nanotechnology, Alagappa University, is acknowledged for assistance with the XRD and Surface Profilometer measurements.

References

[1] Park N.G., van de Lagemaat J., Frank A.J. Comparison of dye-sensitized rutile- and anatase based TiO_2 solar cells. *J. Phys. Chem. D*, 2000, **104**, P. 8989–8994.

[2] Eframoktora R.G. Nelwan, Suliyandi M.M., Prastomo N. Fabrication of anti-reflection coating TiO_2-SiO_2 on silicon substrate with pulsed laser deposition method. *Proc. SPIE*, 2019, Third International Seminar on Photonics, Optics and Its Applications (ISPhoA 2018), 11044N.

[3] Kirillova S.A., Almjashev V.I., Gusarov V.V. Spinodal decomposition in the SiO_2-TiO_2 system and hierarchically organized nanostructures formation. *Nanosystems: Physics, Chemistry, Mathematics*, 2012, **3** (2), P. 100–115.

[4] Ortiz A.A., Yan B., D'Orazio J.A. Ultraviolet radiation, aging and the skin: Prevention of damage by topical cAMP manipulation. *Molecules*, 2014, **19** (5), P. 6202–6219.

[5] Chemin J.B., Bulou S., et al. Transparent anti-fogging and self-cleaning TiO_2/SiO_2 thin films on polymer substrates using atmospheric plasma. *Scientific Reports*, 2018, **8**, P. 1–8.

[6] Mao Q., Zeng D., Xu K., Xie C. Fabrication of porous TiO_2-SiO_2 multifunctional anti-reflection coatings by sol-gel coating method. *RSC Advances*, 2014, **101**, P. 58101–58107.

[7] Dembele A., Rahman M., et al. Deposition of hybrid organic-inorganic composite coatings using an atmospheric plasma jet. system. *J. Nanosci. Nanotechnol.*, 2011, **11**, P. 8730–8737.

[8] Liu F., Shen J., et al. In situ growth of TiO_2/SiO_2 nanospheres on glass substrates via solution impregnation for antifogging. *RSC Advances*, 2017, **7**, P. 15992–15996.

[9] Li X., He J. Synthesis of raspberry-Like SiO_2-TiO_2 nanoparticles toward antireflective and self-cleaning coatings. *ACS Appl. Mater. Interface*, 2013, **5**, P. 5282–5290.

[10] Saxena N., Naik T., Paria S. Organization of SiO_2 and TiO_2 nanoparticles into fractal patterns on glass surface for the generation of superhydrophilicity. *J. Phys. Chem. C*, 2017, **121**, P. 2428–2436.

[11] Venkatesh Y., Dubey R.S., Kumar B. Rapid and economic fabrication of dielectric approach of dielectric reflectors for energy harvesting applications. *Scientific Reports*, 2020, **10**, P. 1–9.

[12] Dubey R.S., Ganesan V. Visible and near-infrared wavelength-selective dielectric reflectors for light management applications. *Superlattices Microstruct.*, 2018, **122**, P. 228–234.

[13] Sedrati H., Benachour M.C., Dehdouh H., Bensaha R. Tuning of the stop-band position in the visible range of SiO_2/TiO_2 Bragg reflectors by doping TiO_2 with transition metals. *Optik*, 2019, **208**, 164098-1-6.

[14] Zhao W., Jia H., et al. Design and realization of antireflection coatings for the visible and the infrared based on mesoporous SiO_2 and SiO_2-TiO_2 hybrid materials. *Appl. Opt.*, 2019, **58** (9), P. 2385–2392.

[15] Dubey R.S., Ganesan V. Reflectance modulation using SiO_2/TiO-multilayer structures prepared by sol-gel spin coating process for optical applications. *Superlattices Microstruct.*, 2017, **111**, P. 1099–1103.

[16] Zhang X., Fujishima A., Jin M., Emeline A.V., Murakami T. Double-layered TiO_2-SiO_2 nanostructured films with self-cleaning and antireflective properties. *J. Phys. Chem. B*, 2006, **110**, P. 25142–25148.

[17] Dalapati G.K., Panah S.M., et al. Color tunable low cost transparent heat reflector using copper and titanium oxide for energy saving application. *Scientific Reports*, 2015, **6**, P. 1–14.

[18] Saravanan S., Dubey R.S. Fabrication and characterization of TiO_2/SiO_2 multilayers using sol-gel spin coating method. *Nanosystems: Physics, Chemistry, Mathematics*, 2019, **10** (1), P. 63–69.

[19] Wu Z.G., Jia Y.R., et al. Core-shell SiO_2/Ag composite spheres: synthesis, characterization and photocatalytic properties. *Materials Science – Poland*, 2016, **34** (4), P. 806–810.

[20] Venkatesh Y., Dubey R.S., Kumar B. Morphological and optical properties of dielectric multilayer structures prepared with distinct precursor concentrations. *Nanosystems: Physics, Chemistry, Mathematics*, 2019, **10** (3), P. 355–360.

[21] Dubey R.S., Krishnamurthy K.V., Singh S. Experimental studies of TiO_2 nanoparticles synthesized by sol-gel and solvothermal routes for DSSCs application. *Results in Physics*, 2019, **14**, 102390-1-6.

[22] Sedrati H., Bensaha R., et al. Correlation between structural and optical properties of SiO_2/TiO_2 multilayers processed by sol-gel technique and applied to Bragg reflectors. *Materials Science*, 2013, **9** (3), P. 113–118.

[23] Xue C., Zhang Q., et al. High photocatalytic activity of Fe3O4-SiO_2-TiO_2 functional particles with core-shell structure. *Journal of Nanomaterials*, 2013, 762423.

[24] Wardiyati S., Adi W.A., Deswita. Synthesis and characterization of microwave absorber SiO_2 by sol-gel method. *IOP Conf. Ser.: Mater. Sci. and Eng.*, 2017, **202**, P. 1–8.

[25] Monshi A., Foroughi M.R., Monsh M.R. Modified Scherrer equation of reaction of reaction to estimate more accurately nano-crystallite size using XRD. *World Journal of Nano Science and Engineering*, 2012, **2**, P. 154–160.

[26] Zhu X., Gu P., et al. Influence of substrate on structural, morphological and optical properties of TiO_2 thin films deposited by reaction magnetron sputtering. *AIP Advances*, 2017, **7**, 125326-1-8.

[27] Barimah E.K., Jones R.P., et al. Phase evolution, morphological, optical and electrical properties of femtosecond pulsed laser deposited TiO_2 thin films. *Scientific Reports*, 2020, **10**, P. 1–12.

[28] Lari N., Ahangarani S., Shanaghi A. Effect of different TiO_2-SiO_2 multilayer coatings applied by sol-gel method on antireflective property. *J. Mater. Eng.*, 2015, **24** (7), P. 2645–2652.

[29] Nezar S., Saoula N., et al. Properties of TiO_2 thin films deposited by RF reactive magnetron sputtering on biased substrates. *Appl. Surf.*, 2017, **395**, P. 172–179.

[30] Klein M.V. *Light Scattering in Solids I, Topics in Applied Physics*, Springer Berlin, Heidelberg, Germany 1983.

[31] Rosales A., Maury-Ramirez A., Det al. SiO_2-TiO_2 coating: synthesis, physical characterization and photocatalytic evaluation. *Coatings*, 2018, **8** (4), P. 1–13.

[32] Popovic D.M., Milosavljevic V., et al. Raman scattering analysis of silicon dioxide single crystal treated by direct current plasma discharge. *Appl. Phys. Lett.*, 2011, **98**, 051503-1-3.